CHINESE OPTICS LETTERS

Vol. 21, No. 11 | November 2023

A universal algorithm for defect-free atomic array with arbitrary periodic geometries [Invited]

Yaoting Zhou (周耀庭)[1], Shaoxiong Wang (王绍雄)[1], Jiayi Chen (陈嘉怡)[1], Yifei Hu (胡逸飞)[1], Zhongxiao Xu (徐忠孝)[1,2*], and Heng Shen (申 恒)[1,2]

[1] State Key Laboratory of Quantum Optics and Quantum Optics Devices, Institute of Opto-electronics, Shanxi University, Taiyuan 030006, China

[2] Collaborative Innovation Center of Extreme Optics, Shanxi University, Taiyuan 030006, China

*Corresponding author: xuzhongxiao@sxu.edu.cn

Received August 2, 2023 | Accepted October 23, 2023 | Posted Online November 9, 2023

The defect-free neutral atom array has emerged as an ideal platform to investigate complex many-body physics of interacting quantum particles, offering the opportunities for quantum simulation and quantum-enhanced metrology. To fast build a large-scale quantum system, we design a sorting-atom algorithm with maximum parallelisms. Compared with previous protocols, our method saves the rearrangement time by sorting row-by-row and is also universal to arbitrary periodic patterns with no need to change the hardware. We present the generation of a defect-free square and other periodic geometries and demonstrate the potential to scale up a defect-free array to 2500 atoms with only about 180 steps of rearrangement.

Keywords: optical tweezer; defect-free atomic array.
DOI: 10.3788/COL202321.110010

1. Introduction

The recent decade has witnessed great developments in the platform of the defect-free array of individually controlled neutral atoms[1-8]. In combination with Rydberg excitation, this system can simulate the many-body behavior of interacting quantum particles, thus enabling applications in the quantum simulation of condensed matter and high-energy physics, quantum optimization, and also quantum-enhanced metrology with nonclassical states of atoms[9–17]. Here, a defect-free periodic pattern of atoms plays essential roles, such as probing the quantum spin liquid states with a Kagome lattice[18]. In general, the spatial light modulator (SLM) or micro lens enables the production of an array of optical microtraps. However, a light-assisted collision blockade impedes the realization of defect-free neutral atomic arrays in such static optical tweezers[19]. To overcome this challenge, an acousto-optic deflector (AOD) was suggested for generating dynamical tweezers to sort the atoms into a target configuration according to the information extracted from the initial image with the atoms stochastically loaded in the static tweezer.

Given the limited atomic lifetime, shortening the rearrangement process with dynamical optical tweezers is in high demand, especially for large scale atomic configurations where the atomic lifetime is inversely proportional to the atomic number N. Currently, most of the sorting-atom algorithms use the one-by-one atom assembling process, such as the heuristic cluster algorithm (HCA)[20], the heuristic path-finding algorithm (HPFA)[21], and the A* searching algorithm (ASA). The HCA proposed by Zhan *et al.* is more efficient than the two other algorithms. Very recently, Chen *et al.* reported a sorting algorithm with a parallel configuration operated on a field programmable gate array (FPGA)[22], which no longer needed to wait for the data transfer from the electron multiplying charge coupled device (EMCCD) to the computer CPU. Unfortunately, if the target pattern is not the square lattice, e.g., a triangle lattice, then their approach requires rotating the two-dimensional AOD by using a specific angle[22,23]. Hence, the accuracy of the rotation angle largely affects its performance. In addition, there are many other algorithms that are based on mobile optical tweezers, such as the compacting algorithm[24], the flicker-free atom controls algorithm[25,26], the linear sum assignment problem (LSAP) algorithm[27], the shortest-move heuristic algorithm[28], and the Hungarian matching algorithm[29].

In this Letter, we propose a parallel algorithm of the sorting-atom process, allowing multiple atoms in the same row (column) to move simultaneously to reduce the time cost of the rearrangement. In contrast to the method in Ref. [14], any physical changes in the hardware, such as AOD rotation, are not needed. Therefore, it is universal to all the periodic configurations like the triangle, hexagonal, and Kagome lattices.

2. Sorting-Atom Technique

2.1. Hardware

The experimental setup is illustrated in Fig. 1(a). A ^{87}Rb atomic cloud in the magneto-optical trap (MOT) is cooled to around 20 μK via polarization gradient cooling[30]. By using an SLM (LCOS-SLM, Hamamatsu X15213) and an objective lens with an NA = 0.5 and a work distance of 14 mm (Mitutoyo G Plan Apo 50×), a static tweezer can be generated. However, the filling rate of the single atom is normally 50%, arising from the collision blockade in the optical micro-dipole-trap[31]. This probability can be increased up to 90% by manipulating the collisions between pairs of trapped atoms[32,33]. However, the occupancy in the atomic array still decreases very quickly with N[14]. To achieve a defect-free array, another movable tweezer array produced by a 2D-AOD (AA Opto-electronic DTSXY-400-850) is applied to realize the rearrangement. Before the rearrangement with this dynamical tweezer, the atomic occupation is first detected by taking the image with the EMCCD (Andor ixon Ultra 897) and transferring it to the computer, where our sorting algorithm designs the rearrangement strategy. An arbitrary waveform generator (AWG, Spectrum m4i.6631-x8) is then instructed to produce the associated multi-frequency signal to drive the AOD. Here, the deflected array of the optical beams from the AOD combined with the static tweezer beams is focused together in the vacuum chamber. The back-reflected fluorescence of the atoms' distribution will be picked up by a dichroic mirror and imaged by an EMCCD.

Figure 1(b) shows the moving process. The atom is first loaded to a dynamical trap with a depth three times deeper than that of the static one, and then is moved to another static trap. When arriving at the target position, the trap depth is ramped down in order to load the atom back into the shallow tweezer. During this procedure, the static tweezers remain in position due to the low refreshing rate of the SLM, while the moveable tweezer can be controlled by radio frequency (RF), which can be refreshed in time and can be programmed to be customized.

2.2. Soldier-like rearrangement

The basic idea of our sorting algorithm is lining up atoms in a row (column) at the same time. Since its logic is similar to soldiers lining up, we call it the soldier-like rearrangement. The detailed process is depicted in Fig. 2. Initially, the atoms in a line are randomly disturbed (top panel). First, we set a point as the center marked with a red triangle in the figure. Supposing n is the size of a target row (column), the center is located at $\lceil n/2 \rceil$ with $x = \lceil \cdot \rceil$ being the ceiling function (for instance, if $n = 10$, $x = 5$ and if $n = 11$, $x = 6$). All the atoms then line up towards the center at the same time. In this process, if the atom is already located at the right position, then there is no action on it. Otherwise, atoms are locally shined with deflected beams from the AOD, leading to the loading of the moveable tweezers and thus one starts moving the atoms. Clearly, as a result of the

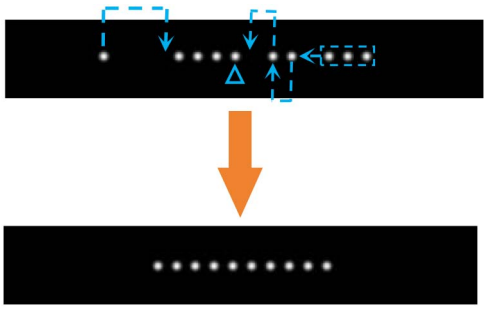

Fig. 2. Example of the soldier-like rearrangement, taking ten randomly distributed trapped atoms in one row as an example. The predefined center is marked as a blue triangle in the upper picture. All the atoms line up towards this center in a line, and the path is labeled with blue arrows. The final pattern is shown in the bottom panel.

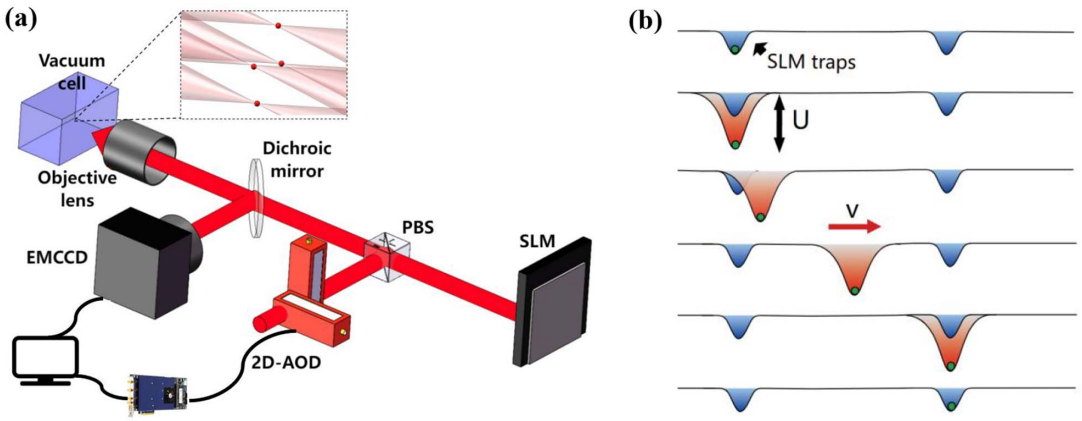

Fig. 1. Schematic of the setup of the two-dimensional defect-free atom arrays. (a) Static and moveable optical tweezers are formed by the SLM and the 2D-AOD, respectively.They combine on the polarization beam splitter (PBS) and then pass through a high NA objective lens, shining on the atoms as an array of optical microtraps. The single atom fluorescence is picked up by a dichroic mirror and imaged by the EMCCD. (b) The mechanism of a single atom moving between static and moveable traps.

parallel approach the time cost is reduced with respect to the sorting process with one-by-one assembly.

Notice that in each movement, the atom first has to be transferred from the shallow trap to the deep one, and when arriving at the target location, the reversed transfer is operated. Consequently, the parallel method also saves the time of the loading transfer, further reducing the total time cost of the rearrangement.

2.3. Algorithm demonstration

We proceed to demonstrate the feasibility of our algorithm by taking a 10×10 square lattice as a target configuration as an example. Assuming the initial 50% filling rate in the static tweezers, we set a size of the target array around 40% of the source array to maximize the rearrangement success rate. Thus, in this case, the source array is a 16×16 square pattern.

The sorting cycle is outlined in Fig. 3 and summarized as follows.

(1) **Mapping process.** First, one generates the coordinates associated with the target defect-free configuration, so-called source coordinates. By taking the image of the fluorescence with the EMCCD, the atom positions are obtained directly, and then mapped to the predefined source coordinates. By comparison, the atomic occupation in the static tweezers is evaluated. Most importantly, the source coordinates include a list of drive frequencies to control the AOD, corresponding to each target atomic position. Therefore, owing to this image, one knows which atoms are already located in the target position, and the associated AOD frequencies should be off. Otherwise, they have to be moved to the target positions by varying the 2D-AOD drive frequencies to the predefined values in accordance with the target positions.

(2) **Running the sorting algorithm.** In this step, the moving paths based on the source array are designed following the preset rearrangement rules.

(3) **Calculating and applying the waveforms.** According to the moving paths, the waveforms are achieved. All the waveforms will be combined into a complete waveform that contains all the moving behaviors. This waveform is sent to the AOD, and one operates the sorting-atom process. It is noted that random phases have to be applied when calculating the waveform, aiming to suppress the intermodulation.

(4) **Making a judgment.** Another picture is taken to judge if the sorting is completed. If not, then a new cycle is triggered and the above steps are repeated. If the lattices are filled, then one more step is applied to kick off all the unnecessary atoms.

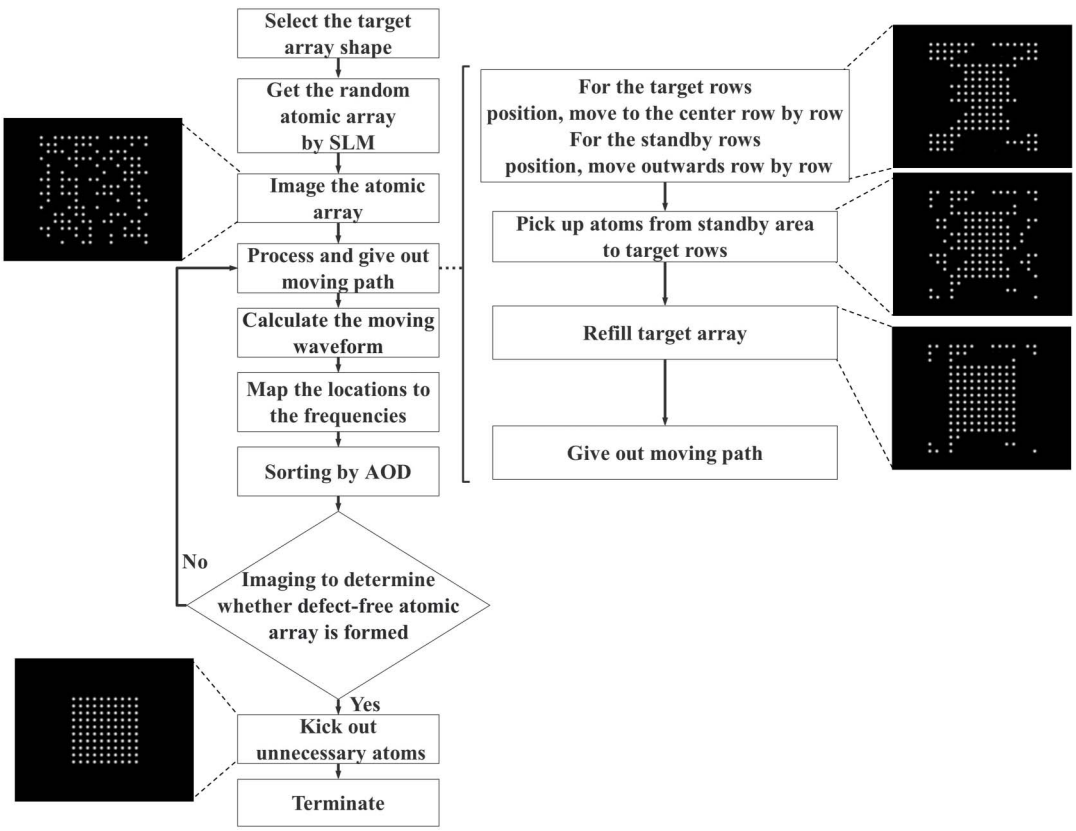

Fig. 3. Flowchart of the soldier-like algorithm. Sorting process is implemented from up to down.

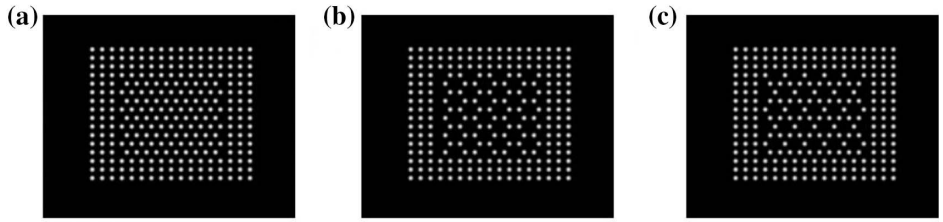

Fig. 4. Experimental generation of (a) the triangle lattice, (b) the hexagonal lattice, and (c) the Kagome lattice. The patterns include two areas, a target area and a standby area. The standby array is used for refilling the target array. The standby array is designed as a rectangular array that is suitable for soldier-like rearrangement.

We should also emphasize the importance of the standby rows. Given a 16×16 source array and a 10×10 target lattice, the first three rows and the last three rows are left, referred to as standby rows, and moved to the corners, as shown in Fig. 3. The rest of the ten rows are target rows in the central area where the rearrangement implies the soldier-like sorting algorithm. However, if the atom number in the ith target row is not enough to build the ideal configuration, then the atoms in the standby rows nearby will be moved to fill this row. This rearrangement is implemented row by row.

From the experimental side, different types of periodic lattices could be required for specific project designs, such as a triangle lattice, hexagonal lattice, or Kagome lattice. All these lattices can be treated as a square lattice but with different mapping coordinates. If changing the lattice structures for each different experiment, then one just needs to choose a different SLM pattern but apply the same algorithm. Figure 4 shows the experimental generation of the triangle, hexagonal, and Kagome lattices with the standby rows left in the corners.

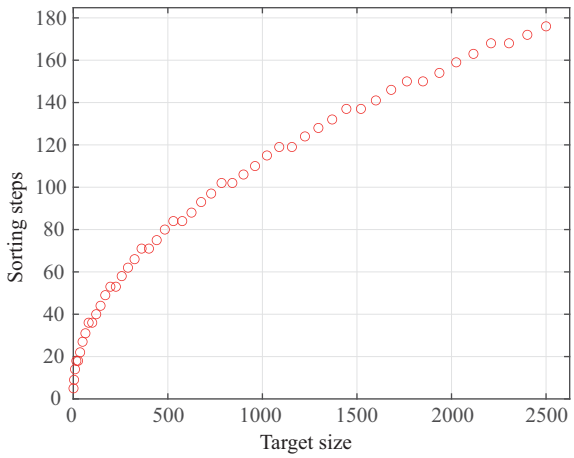

Fig. 5. Sorting steps as a function of the target number in the rearrangement of the square lattice.

3. Analysis and Discussion

Sorting time is the key factor in the sorting-atom process. The trap lifetime of the atoms is typically around 20 seconds. To realize the sorting within the limited lifetime, moving steps need to be as few as possible and the moving distance also needs to be as short as it can be. When the array size is small, the Hungarian matching algorithm and some other algorithms show great advantage[27,29]. These algorithms move atoms one by one with fast and efficient calculation. However, as for a large scale, one-by-one atom assembling takes too much time. The paralleled algorithm is a potential method that can be used to decrease the sorting time by largely reducing the number of sorting steps. In our proposal, the parallelism degree is the maximum. Figure 5 gives the sorting steps as a function of the target array size. Here, to increase the success probability we set the size ratio of the target to the source as 40%. This is ten percent less than the single atom filling rate. As shown in Fig. 5, we find that even when the target array size is 2500, only around 180 steps are required to realize the defect-free square lattice.

Consider an $m \times m$ source array and an $n \times n$ target lattice, i.e., $\frac{n \times n}{m \times m} \approx 40\%$. As illustrated in Fig. 6, the m steps are required at first, including the sorting process in the target rows (n) and also the rearrangement of the standby rows ($m - n$), to form the rectangular pattern. We assume that the atom number in each target row is not enough to build the defect-free configuration. Thus, the $m - n$ steps are needed to move the atom in the standby area to the target row along the vertical direction.

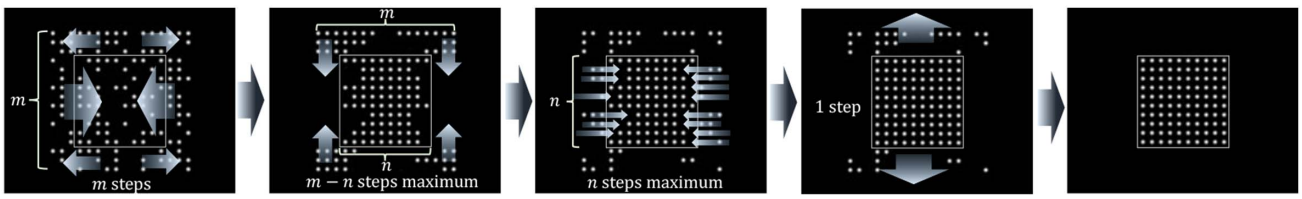

Fig. 6. Illustration of the sorting process to evaluate the steps in the rearrangement of the square lattice.

Lastly, n steps are implemented to refill the target array. In summary, the maximum step number of one cycle is $2m$. Actually, it is possible that one fails the rearrangement and has to start a new cycle attributed to the atom loss and limited standby atoms. Here, one has to make a decision. If more than $0.1 \times 2m$ steps are required in the second cycle, then we think the atom loss is too serious, and an optimization of moving strategy is in high demand. After two cycles of the sorting-atom process, one more step is needed to kick out all of the unnecessary atoms. In this case, the maximum number of sorting steps is $2m \times (1 + 0.1) + 1$.

In addition, subject to the working principle of the 2D-AOD when the drive frequencies (x_1, y_1) and (x_2, y_2) are applied for two deflected beams, two unwanted beams corresponding to frequencies (x_1, y_2) and (x_2, y_1) are also produced. Consequently, it is nearly impossible for a randomly filled atom array to parallelly sort by both horizontal and vertical directions simultaneously. The row-by-row sorting process thus keeps the maximum parallelism degree.

4. Conclusion

In conclusion, we develop a sorting-atom algorithm to build large scale defect-free atomic arrays with optical tweezers and demonstrate its feasibility by generating square, triangle, hexagonal, and Kagome lattices. It is common knowledge that moving atoms may cause heating. So most algorithms[8,20–29] are searching for the shortest moving distance. In our parallel algorithm, much less steps are needed at the expense of enlarging the moving distance. This algorithm has great superiority when array size is large. For example, the moving steps of a 1000 target array is ~500 for the HPFA[21], while it only needs ~100 steps for our algorithm. So our algorithm can save ~80% time for a 1000 target array. However, each coin has two sides. More atoms are moved in our algorithm. The advantage is that the moving duration can be greatly reduced, while the disadvantage is unavoidable atom heating and loss. So some further cooling methods, like gray molasses[34], are needed to close this loophole.

This so-called soldier-like algorithm keeps the maximum parallelism degree, leading to the reduction of sorting time, while the special atomic "addressing" mode allows for producing any arbitrary periodic geometries. Our method can be directly applied to quantum simulation of condensed-matter physics such as frustrated magnetism in many-body system, and also offers the possibility of entanglement-enhanced quantum sensing and metrology.

Acknowledgement

This work was supported by the National Key R&D Program of China (No. 2020YFA0309400), the National Natural Science Foundation of China (Nos. 12222409, 12174081, and 11974228), and the Key Research and Development Program of Shanxi Province (No. 202101150101025). H. S. acknowledges the financial support from the Royal Society Newton International Fellowship Alumni (AL201024).

References

1. A. Omran, H. Levine, A. Keesling, G. Semeghini, T. T. Wang, S. Ebadi, H. Bernien, A. S. Zibrov, H. Pichler, S. Choi, J. Cui, M. Rossignolo, P. Rembold, S. Montangero, T. Calarco, M. Endres, M. Greiner, V. Vuletić, and M. D. Lukin, "Generation and manipulation of Schrödinger cat states in Rydberg atom arrays," Science **365**, 570 (2019).
2. P. Kómár, T. Topcu, E. M. Kessler, A. Derevianko, V. Vuletić, J. Ye, and M. D. Lukin, "Quantum network of atom clocks: a possible implementation with neutral atoms," Phys. Rev. Lett. **117**, 060506 (2016).
3. T. M. Graham, Y. Song, J. Scott, C. Poole, L. Phuttitarn, K. Jooya, P. Eichler, X. Jiang, A. Marra, B. Grinkemeyer, M. Kwon, M. Ebert, J. Cherek, M. T. Lichtman, M. Gillette, J. Gilbert, D. Bowman, T. Ballance, C. Campbell, E. D. Dahl, O. Crawford, N. S. Blunt, B. Rogers, T. Noel, and M. Saffman, "Multi-qubit entanglement and algorithms on a neutral-atom quantum computer," Nature **604**, 457 (2022).
4. D. Barredo, V. Lienhard, S. De Léséleuc, T. Lahaye, and A. Browaeys, "Synthetic three-dimensional atomic structures assembled atom by atom," Nature **561**, 79 (2018).
5. Y. Liu, Z. Wang, P. Yang, Q. Wang, Q. Fan, S. Guan, G. Li, P. Zhang, and T. Zhang, "Realization of strong coupling between deterministic single-atom arrays and a high-finesse miniature optical cavity," Phys. Rev. Lett. **130**, 173601 (2023).
6. S. J. Evered, D. Bluvstein, M. Kalinowski, S. Ebadi, T. Manovitz, H. Zhou, S. H. Li, A. A. Geim, T. T. Wang, N. Maskara, H. Levine, G. Semeghini, M. Greiner, V. Vuletic, and M. D. Lukin, "High-fidelity parallel entangling gates on a neutral atom quantum computer," arXiv:2304.05420 (2023).
7. J. W. Lis, A. Senoo, W. F. McGrew, F. Rönchen, A. Jenkins, and A. M. Kaufman, "Mid-circuit operations using the omg-architecture in neutral atom arrays," arXiv:2305.19266 (2023).
8. S. Ebadi, T. T. Wang, H. Levine, A. Keesling, G. Semeghini, A. Omran, D. Bluvstein, R. Samajdar, H. Pichler, W. W. Ho, S. Choi, S. Sachdev, M. Greiner, V. Vuletić, and M. D. Lukin, "Quantum phases of matter on a 256-atom programmable quantum simulator," Nature **595**, 227 (2021).
9. A. W. Glaetzle, R. M. W. van Bijnen, P. Zoller, and W. Lechner, "A coherent quantum annealer with Rydberg atoms," Nat. Commun. **8**, 15813 (2017).
10. A. Browaeys, D. Barredo, and T. Lahaye, "Experimental investigations of dipole–dipole interactions between a few Rydberg atoms," J. Phys. B At. Mol. Opt. Phys. **49**, 152001 (2016).
11. S. Lloyd, "Universal quantum simulators," Science **273**, 1073 (1996).
12. I. M. Georgescu, S. Ashhab, and F. Nori, "Quantum simulation," Rev. Mod. Phys. **86**, 153 (2014).
13. H. Bernien, S. Schwartz, A. Keesling, H. Levine, A. Omran, H. Pichler, S. Choi, A. S. Zibrov, M. Endres, M. Greiner, V. Vuletic, and M. D. Lukin, "Probing many-body dynamics on a 51-atom quantum simulator," Nature **551**, 579 (2017).
14. A. Browaeys and T. Lahaye, "Many-body physics with individually controlled Rydberg atoms," Nat. Phys. **16**, 132 (2020).
15. A. W. Young, W. J. Eckner, W. R. Milner, D. Kedar, M. A. Norcia, E. Oelker, N. Schine, J. Ye, and A. M. Kaufman, "Half-minute-scale atomic coherence and high relative stability in a tweezer clock," Nature **588**, 408 (2020).
16. G. Bornet, G. Emperauger, C. Chen, B. Ye, M. Block, M. Bintz, J. A. Boyd, D. Barredo, T. Comparin, F. Mezzacapo, T. Roscilde, T. Lahaye, N. Y. Yao, and A. Browaeys, "Scalable spin squeezing in a dipolar Rydberg atom array," arXiv:2303.08053 (2023).
17. W. J. Eckner, N. D. Oppong, A. Cao, A. W. Young, W. R. Milner, J. M. Robinson, J. Ye, and A. M. Kaufman, "Realizing spin squeezing with Rydberg interactions in a programmable optical clock," arXiv:2303.08078 (2023).
18. G. Semeghini, H. Levine, A. Keesling, S. Ebadi, T. T. Wang, D. Bluvstein, R. Verresen, H. Pichler, M. Kalinowski, R. Samajdar, A. Omran, S. Sachdev, A. Vishwanath, M. Greiner, V. Vuletić, and M. D. Lukin, "Probing topological spin liquids on a programmable quantum simulator," Science **374**, 1242 (2021).

19. E. Urban, T. A. Johnson, T. Henage, L. Isenhower, D. D. Yavuz, T. G. Walker, and M. Saffman, "Observation of Rydberg blockade between two atoms," Nat. Phys. **5**, 110 (2009).
20. C. Sheng, J. Hou, X. He, P. Xu, K. Wang, J. Zhuang, X. Li, M. Liu, J. Wang, and M. Zhan, "Efficient preparation of two-dimensional defect-free atom arrays with near-fewest sorting-atom moves," Phys. Rev. Res. **3**, 023008 (2021).
21. D. Barredo, S. De Léséleuc, V. Lienhard, T. Lahaye, and A. Browaeys, "An atom-by-atom assembler of defect-free arbitrary two-dimensional atomic arrays," Science **354**, 1021 (2016).
22. S. Wang, W. Zhang, T. Zhang, S. Mei, Y. Wang, J. Hu, and W. Chen, "Accelerating the assembly of defect-free atomic arrays with maximum parallelisms," Phys. Rev. Appl. **19**, 054032 (2023).
23. W. Tian, W. J. Wee, A. Qu, B. J. M. Lim, P. R. Datla, V. P. W. Koh, and H. Loh, "Parallel assembly of arbitrary defect-free atom arrays with a multitweezer algorithm," Phys. Rev. Appl. **19**, 034048 (2023).
24. J. Vala, A. V. Thapliyal, S. Myrgren, U. Vazirani, D. S. Weiss, and K. B. Whaley, "Perfect pattern formation of neutral atoms in an addressable optical lattice," Phys. Rev. A **71**, 032324 (2005).
25. H. Kim, W. Lee, H.-G. Lee, H. Jo, Y. Song, and J. Ahn, "*In situ* single-atom array synthesis using dynamic holographic optical tweezers," Nat. Commun. **7**, 13317 (2016).
26. W. Lee, H. Kim, and J. Ahn, "Three-dimensional rearrangement of single atoms using actively controlled optical microtraps," Opt. Express **24**, 9816 (2016).
27. K.-N. Schymik, V. Lienhard, D. Barredo, P. Scholl, H. Williams, A. Browaeys, and T. Lahaye, "Enhanced atom-by-atom assembly of arbitrary tweezer arrays," Phys. Rev. A **102**, 063107 (2020).
28. D. Ohl de Mello, D. Schäffner, J. Werkmann, T. Preuschoff, L. Kohfahl, M. Schlosser, and G. Birkl, "Defect-free assembly of 2D clusters of more than 100 single-atom quantum systems," Phys. Rev. Lett. **122**, 203601 (2019).
29. W. Lee, H. Kim, and J. Ahn, "Defect-free atomic array formation using the Hungarian matching algorithm," Phys. Rev. A **95**, 053424 (2017).
30. H. J. Metcalf and P. van der Straten, *Laser Cooling and Trapping* (Springer, 1999).
31. N. Schlosser, G. Reymond, I. Protsenko, and P. Grangier, "Sub-poissonian loading of single atoms in a microscopic dipole trap," Nature **411**, 1024 (2001).
32. T. Grünzweig, A. Hilliard, M. McGovern, and M. F. Andersen, "Near-deterministic preparation of a single atom in an optical microtrap," Nat. Phys. **6**, 951 (2010).
33. B. J. Lester, N. Luick, A. M. Kaufman, C. M. Reynolds, and C. A. Regal, "Rapid production of uniformly filled arrays of neutral atoms," Phys. Rev. Lett. **115**, 073003 (2015).
34. M. O. Brown, T. Thiele, C. Kiehl, T.-W. Hsu, and C. A. Regal, "Gray-molasses optical-tweezer loading: controlling collisions for scaling atom-array assembly," Phys. Rev. X **9**, 011057 (2019).